Solvent-free solution processed passivation layer for improved long-term stability of organic field-effect transistors†

Sooji Nam,[a] Jaeyoung Jang,[a] Kihyun Kim,[b] Won Min Yun,[a] Dae Sung Chung,[a] Jihun Hwang,[a] Oh Kwan Kwon,[a] Taihyun Chang[b] and Chan Eon Park*[a]

Received 31st March 2010, Accepted 27th September 2010
DOI: 10.1039/c0jm00898b

In an effort to realize organic field-effect transistors (OFETs) that are stable over long periods of time, we have designed an organic–inorganic hybrid passivation material (TGD622t) prepared *via* a non-hydrolytic sol–gel process that does not require the use of solvents. Fourier-transform infrared spectroscopy, atomic force microscopy, and UV-visible spectroscopy demonstrated the high density and low porosity of the organic–inorganic hybrid transparent TGD622t film after low-temperature curing (below 100 °C). The dense TGD622t passivation layer, which exhibited a water vapor transmission rate (WVTR) of 0.434 g m^{-2} per day, effectively protected the poly[9,9-dioctylfluorenyl-2,7-diyl]-*co*-(bithiophene)]-based OFETs from humidity and oxygen in ambient air, resulting in a much more robust OFET performance with long-term stability relative to the operation of unpassivated devices.

Introduction

Recently, considerable effort has been devoted to improving the environmental stability of organic electronics, the electrical properties of which degrade significantly over time in the presence of water and oxygen in ambient air.[1–4] Therefore, the introduction of a passivation layer is necessary to protect devices from the effects of water and oxygen. The two methods that are primarily used to introduce a passivation layer are vacuum deposition and solution deposition. To date, vacuum deposition processes, such as atomic layer deposition (ALD) and chemical vapor deposition (CVD), have been predominantly used to produce passivation layers that function as barriers. Although inorganic thin film passivation layers prepared by ALD or CVD processes and polymer/inorganic multilayers produce good protection barriers against water and oxygen,[5–7] lengthy processing times and high costs inhibit their widespread commercial application. Solution deposition processes, however, are simple, low-cost solutions that reduce the required processing time.[8,9]

In general, solution-processed organic passivation layers show poor barrier properties relative to vacuum-deposited inorganic films due to the large number of defects or pinholes present in the films.[10] High-temperature or UV crosslinking processes are necessary to improve the film density and barrier properties. For several decades, organic–inorganic hybrid materials prepared by sol–gel processes have attracted interest on account of their easy processability (solution processability and low curing temperature) and high barrier properties.[9,11–13] Organic–inorganic network structures produced by polycondensation between organic and inorganic components combine the advantages of both organic and inorganic materials. However, the hydrolysis and condensation reactions that occur during the sol–gel preparation of materials in conjunction with the hydrolytic process are so rapid that abrupt volume shrinkage is observed in the films.[14] Additionally, residual Si–OH groups produced by the hydrolysis reaction cannot be completely condensed to Si–O–Si groups during the hydrolytic sol–gel process.[15] The non-hydrolytic (NH) sol–gel process, which does not require solvents such as water or alcohol, does not experience volume shrinkage because the reaction rates are moderate. These conditions convey several advantages to the sol–gel process: it is low in cost, simple, and requires a low curing temperature (below 100 °C).[16–18]

In the present study, we designed and characterized solution processed organic–inorganic hybrid passivation materials by the NH sol–gel process. The NH sol–gel process was used to fabricate a transparent film with excellent barrier properties, even when used with a solvent-free low-temperature curing process. Finally, we applied this film as a passivation layer to enhance the lifetimes of organic field-effect transistors (OFETs), resulting in long-term stable OFET operation relative to unpassivated OFETs.

Experimental

Preparation and characterization of materials

3-Glycidoxypropyltrimethoxysilane (GPTMS, ≥98%, purchased from Aldrich) was adopted to promote the formation of networks by presenting peroxide groups, and tetraethyl orthosilicate (TEOS, reagent grade, 98%, purchased from Aldrich) was used as the inorganic precursor. Barium hydroxide monohydrate ($Ba(OH)_2 \cdot H_2O$, purchased from Aldrich) and diphenylsilanediol (DPSD, 95%, purchased from Aldrich), as the catalyst and reactive reagent, respectively, induced the condensation reaction. The addition of titania, prepared from titanium propoxide

[a]*Polymer Research Institute, Department of Chemical Engineering, Pohang University of Science and Technology (POSTECH), Pohang, 790-784, Korea. E-mail: cep@postech.ac.kr; Fax: +82-54-279-8298; Tel: +82-54-279-2269*
[b]*Polymer Physical Chemistry Laboratory, Department of Chemistry, Pohang University of Science and Technology (POSTECH), Pohang, 790-784, Korea*

† Electronic supplementary information (ESI) available: further experimental details. See DOI: 10.1039/c0jm00898b

($Ti(OC_3H_7)_4$, 98%, purchased from Aldrich), increased the film densities at low temperatures. Titania catalyzes inorganic condensations and epoxide polymerizations.[19] The structures of TEOS, GPTMS, DPSD, and $Ti(OC_3H_7)_4$ are shown in Fig. 1(a). A NH hydrolytic sol–gel material was prepared by mixing TEOS, GPTMS, and DPSD in a ratio of 60 mol% : 20 mol% : 20 mol% (to form the material referred to here as TGD622), in the following manner: TEOS and GPTMS were first mixed; $Ba(OH)_2 \cdot H_2O$ (0.75 mol%) and DPSD were added sequentially; the solution was stirred continuously at 90 °C for 4 h. Finally, the solution was cooled to room temperature under constant stirring. Titania was prepared separately according to the following procedure:[20] 9.0 mL titanium propoxide and 0.27 mL acetylacetone (or 2,4-pentanedione, ReagentPlus®, ≥99%, purchased by Aldrich) as a chelating agent were mixed for 15 min. To this solution were sequentially added, with stirring, 0.20 mL 2-propanol (ReagentPlus®, ≥99%, purchased from Aldrich) and 0.075 mL glacial acetic acid (99.8%, purchased from Aldrich). The titania sol was allowed to react for 1 h. Subsequently, 10 mol% titania was added to the TGD622 solution and allowed to react for 2 h at room temperature. The final passivation material was named TGD622t (t for titania). A schematic illustration of the TGD622t preparation process is shown in Fig. 1(b). The structure of TGD622 was characterized by matrix-assisted laser desorption and ionization time-of-flight mass spectroscopy (MALDI-TOF MS, Bruker REFLEX™ III). The matrix used for the MALDI-TOF experiment, *trans*-3-indolacrylic acid (IAA, 98%, purchased from Aldrich) was dissolved in acetone at 80 mg mL^{-1}. The IAA and TGD622 solutions were mixed at a 4 : 1 ratio (matrix : analyte, v/v). The mixed solution was dropped onto the MALDI plate and air-dried. Films of TGD622t were analyzed by Fourier transform infrared (FTIR) spectroscopy (Nicoret 6700, Thermo Elec. Co), atomic force microscopy (AFM) (Digital Instrument Multimode SPM), a contact angle meter (SEO 300A, SEO Co.), UV–Vis–NIR spectroscopy (UV–Vis, Cary 5000, Varian Co.), and water vapor transmission rate (WVTR) analysis (Permatran-W 3/33 MA). (100) Oriented p-type Si wafers with a specific resistivity of 1–20 Ω cm^{-1} were used as substrates for the FTIR, AFM and contact angle measurements. Glass slides and poly(ethylene terephthalate) (PET) films were used as substrates for UV–Vis and WVTR measurements, respectively. Si wafer was cleaned in piranha solution at a 7 : 3 ratio (sulfuric acid : hydrogen peroxide, v/v), rinsed with de-ionized water and dried with nitrogen gas before use. Glass slides were ultrasonically cleaned in acetone (CMOS™, 99.5%) and 2-propanol, respectively, and dried with nitrogen gas. The TGD622 and TGD622t were spin-coated at 4500 rpm in air and TGD622t films were cured in air at different temperatures (90 °C, 200 °C and 350 °C, respectively). Finally, resulting films were stored in a vacuum desiccator before measurements were taken. In contact angle measurements, we used de-ionized water as a solvent for measuring the static contact angle and 5-time measurements were performed for averaging the data. A surface profiler (Alpha-step® 500, KLA Tencor) was used for measuring the thickness of the films.

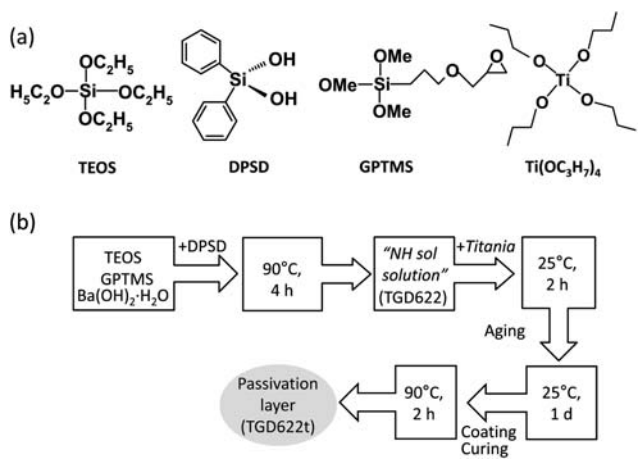

Fig. 1 (a) Chemical structures of TEOS, GPTMS, $Ti(OC_3H_7)_4$, and DPSD used in the synthesis of NH sol–gel hybrid materials. (b) Schematic drawing of the preparation process for TGD622t.

Device fabrication and measurements

The OFETs were fabricated using a heavily-doped Si wafer as the gate substrate. Thermally grown 300 nm thick SiO_2 was used as the gate dielectric (modified with octadecyltrichlorosilane (ODTS)). Subsequently, a solution of poly[9,9-dioctylfluorenyl-2,7-diyl]-*co*-(bithiophene)] (F8T2) (0.5 wt%) in chloroform was spin-cast in air at 2000 rpm, and the devices were post-heated in air at 70 °C on a hot plate for 30 min to eliminate the residual solvent. The top-contact geometry OFETs were formed by depositing the source/drain electrodes onto the active layer *via* thermal evaporation of gold through a shadow mask. Then 100 nm thick gold was deposited under high vacuum (1×10^{-6} torr) at a deposition rate of 10 Å s^{-1}. The channel widths (W) and lengths (L) were 1500 μm and 100 μm, respectively. The field-effect mobility (μ) and threshold voltage (V_{th}) were obtained from the slope of a plot of the square root of the drain current (I_D) *versus* the gate voltage (V_G) in the saturation regime using the equation $I_D = (WC_i/2L)\mu(V_G - V_{th})^2$, where I_D is the drain current, C_i is the capacitance per unit area of dielectrics (10 nF cm^{-2} at 100 kHz), and V_{th} is the threshold voltage in ambient air at room temperature. The electrical characteristics of the F8T2-based OFETs were measured in dark air with Keithley 2400 and 236 source/measure units, and the C_i values were characterized using a 4284A LCR meter (Agilent Tech.) The 800 nm thick TGD622t passivation material was spin-coated onto the OFETs at 4500 rpm, and the device with the passivation layer was cured in air at 90 °C for 2 h on a hot plate.

Results and discussion

The organic–inorganic hybrids of TEOS, GPTMS, and DPSD (TGD622) were synthesized by the NH sol–gel process to form siloxane (Si–O–Si) networks. MALDI-TOF MS was used to characterize the material structure and identify the main molecular species present in TGD622; the average molecular weight (W_m) was also calculated.[21] Fig. 2 shows the MALDI-TOF mass spectrum of TGD622, and the inset of Fig. 2 presents the structure of TGD622. The main species present in TGD622 corresponded to a pentamer (the calculated W_m was 834), which was consistent with the molar ratio of TGD622 (TEOS : GPTMS : DPSD = 3 : 1 : 1). Periodic MALDI-TOF

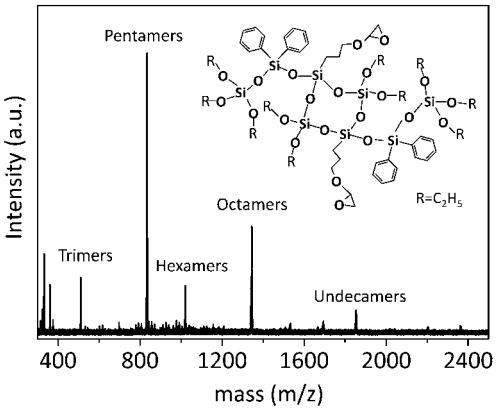

Fig. 2 MALDI-TOF mass spectrum of TGD622. The inset shows the structure of liquid TGD622.

peaks, at intervals of 510, indicated that molecular species in the TGD622 material differed by the mass of the trimer unit. The main molecular structures in TGD622 were composed of trimers, pentamers, hexamers, octamers, and undecamers. However, because the W_m of the liquid TGD622 determined by MALDI-TOF MS was small, TGD622 failed to form a dense film after spin-coating. Therefore, titania was added to the sol–gel solution to increase the film density (TGD622t) because titania can promote inorganic condensation and epoxide polymerization.[19]

Fig. 3(a) shows the FTIR spectra of TGD622 (black line) and TGD622t cured at 90 °C (gray line) for 2 h, respectively. Fig. 3(b) shows a detailed view of the spectra over the range 1200–800 cm^{-1}. TGD622t demonstrated the inorganic condensation of Si–O–Ti as well as Si–O–Si bonds. An intense band around 1100 cm^{-1} was detected in both TGD622 and TGD622t and was attributed to the asymmetric stretching vibration of Si–O–Si bonds.[22] A new band across the range 950–930 cm^{-1} in the TGD622t spectrum was assigned to the Si–O–Ti bonds.[23,24] The appearance of Si/Ti binary oxide bands in the TGD622t spectrum indicated that the siloxane matrices were connected by titania, which increased the W_m. The FTIR spectrum of TGD622t, shown in Fig. 3(b), presented epoxide bands at 960 cm^{-1} and 820 cm^{-1} with slightly lower intensities than those of TGD622, indicating that the epoxide rings had opened.[25] In Fig. 3(a), although TGD622t presented a band over the range 3400–3000 cm^{-1} (indicating unreacted Ti–OH or Si–OH), TGD622t exhibited hydrophobic properties; the inset in Fig. 3(a) shows the water contact angles of the TGD622 (68 ± 1°) and TGD622t (90 ± 2°) films, respectively. The hydrophobic surface property of TGD622t was correlated with the extent of the condensation reaction that produced the amorphous Si–O–Si or Si–O–Ti networks.[9] A comparison of the FTIR spectra demonstrated that titania enhanced the inorganic and organic networks *via* inorganic condensation with the concomitant epoxide ring opening polymerization, thereby producing more dense TGD622t films than was possible for the TGD622 films.

Fig. 4 shows the FTIR spectra of TGD622t cured at various temperatures for 2 h. In TGD622t cured at 200 °C, it was observed that the spectra were almost the same as those of TGD622t cured at 90 °C, except that the C–H stretching and symmetric bending absorptions at 2980 cm^{-1} and 1390 cm^{-1}, respectively, were slightly decreased. This decrement was probably due to the partial decomposition of organic compounds with heat treatment.[26] For TGD622t cured at 350 °C, organic compounds were mostly combusted: C–H stretching absorption bands in the range of 3000–2850 cm^{-1} and C–H bending (both symmetric and asymmetric) absorptions at 1430 cm^{-1} and 1390 cm^{-1} were remarkably reduced. Furthermore, C–O stretching bands in 1130 cm^{-1} and aromatic C=C stretching absorptions in 1600 cm^{-1} and 1480 cm^{-1} were also significantly decreased.[27] These results were confirmed by measuring the changes of film thickness with different heat treatment. The thickness of TGD622t films cured at 90 °C, 200 °C, and 350 °C were found to be 790, 650 and 400 nm, respectively, and the corresponding height profiles are shown in Fig S1 in the ESI†.

Fig. 5(a)–(c) shows AFM images of a TGD622t films cured at 90 °C, 200 °C, and 350 °C, respectively. AFM surface characterization of the TGD622t films permitted study of the surface morphology. The root mean square (r.m.s.) surface roughnesses of TGD622t films in Fig. 5(a)–(c) were found to be 9.6, 11.6 and 7.2 nm, respectively. The film cured at 90 °C showed comparatively macro-pore free and uniform morphology, while the film

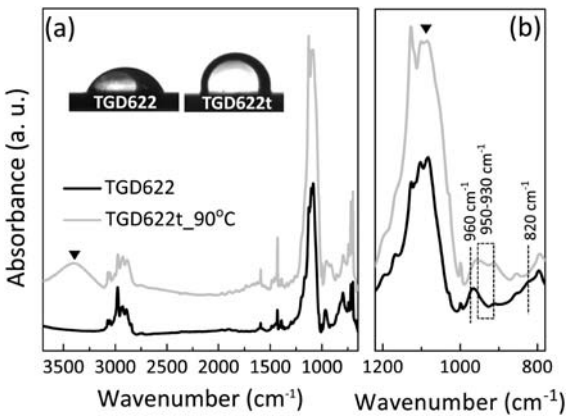

Fig. 3 (a) FTIR spectra of TGD622 and TGD622t cured at 90 °C, and (b) the detailed spectra in the range 800–1200 cm^{-1}. Black and gray lines indicate the spectra of TGD622 and TGD622t, respectively. The inset of (a) shows the water contact angles of the TGD622 and TGD622t films on Si wafers.

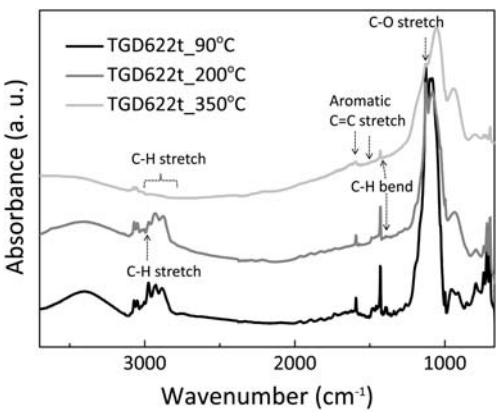

Fig. 4 FTIR spectra of TGD622t cured at 90 °C, 200 °C, and 350 °C, respectively.

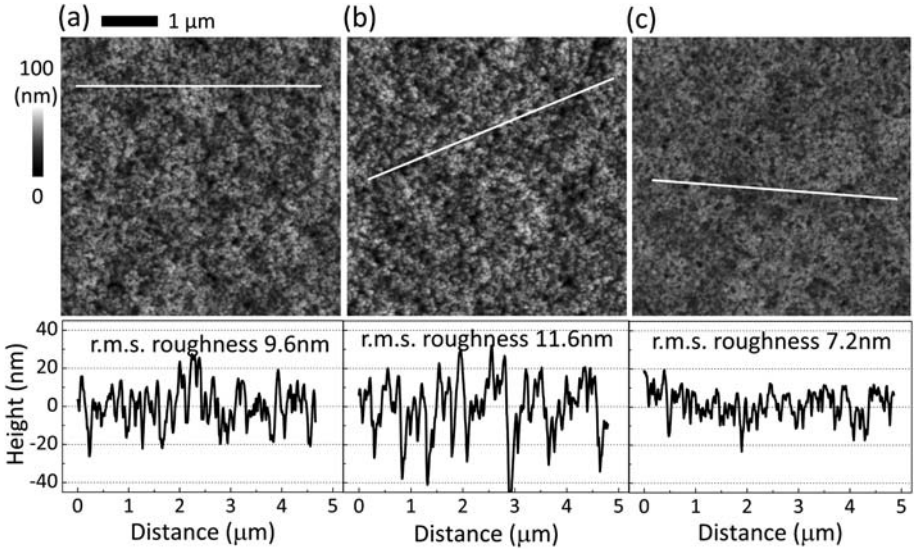

Fig. 5 AFM images and cross-sectional height profiles (bottom panels) of TGD622t cured at (a) 90 °C, (b) 200 °C, and (c) 350 °C, respectively. Here, all images use the same horizontal and vertical scale bars. In bottom panels, r.m.s. means root mean square.

cured at 200 °C showed relatively porous and large surface roughness because parts of the organic compounds were incompletely decomposed. The film cured at 350 °C (see Fig. 5(c)) showed more uniform morphology as well as relatively small r.m.s. surface roughness than those of the films at 90 °C and 200 °C. It is believed that condensed film was formed as organic compounds were removed. It is well known that purely inorganic sol–gel processed materials with high temperature heat treatment have very dense and uniform structure. Although they will have good barrier properties, high temperature processes above 200 °C are not appropriate in OFETs applications, considering that heat treatment at ultra high temperature may directly damage or degrade the organic materials of organic devices. The TGD622t film showed a macropore-free dense morphology, because its organic groups sufficiently filled the pore interstices between the inorganic oxide chains. The AFM results were supported by analysis of the TGD622t (cured at 90 °C) surface by energy dispersive spectrometry (See Fig. S2 in the ESI†). Fig. S2 shows that the atoms Si, O, C, and Ti (which comprised the TGD622t) were uniformly distributed throughout the matrix. Therefore, TGD622t cured at 90 °C formed a uniform and dense film without aggregates.

Fig. 6 shows the UV–Vis transmission spectra of the TGD622t films cured at different temperatures mounted on a glass substrate. The TGD622t film cured at 90 °C showed transmittance properties that were comparable to those of bare glass (black line), except in the UV range 200–350 nm. The films baked at high temperatures exhibited significantly higher absorption in the visible region due to the decomposition of organic compounds.[26] In our system, because the 90 °C heat-treated TGD622t was homogeneous and macropore-free, it showed a high transmittance in the visible region. Furthermore, the TGD622t film showed good UV-blocking abilities (large absorption in the UV region) and, therefore, it may be used as a UV-blocking buffer layer.

Table 1 and Fig. S3† show the water vapor transmission rates (WVTR) of a TGD622t-coated PET film (cured at 90 °C) and

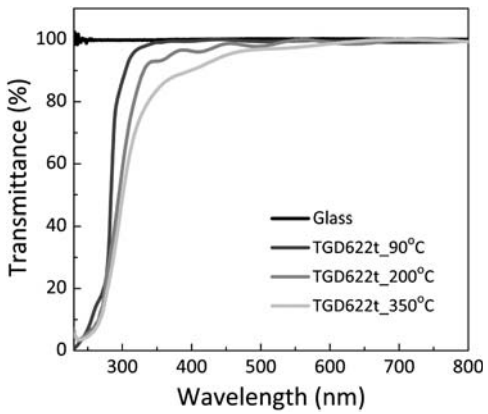

Fig. 6 UV–Vis transmission spectra of TGD622t films cured at different temperatures on glass.

a thermally evaporated SiO_x-coated PET film. The WVTRs of the TGD622t-coated PET film and the thermally evaporated SiO_x coating were 0.434 g m^{-2} per a day and 0.254 g m^{-2} per a day, respectively. The solution-processed TGD622t film showed a comparable WVTR with the thermally evaporated SiO_x film, exhibiting good barrier properties. The barrier robustness of TGD622t was measured by applying a TGD622t film as a passivation layer onto F8T2-based OFETs (see the inset

Table 1 Thickness values and water vapor transmission rates (WVTR) of the TGD622t-coated PET film and the thermally evaporated SiO_x-coated PET film

	TGD622t on PET	Thermally evaporated SiO_x on PET
thickness/nm	800–1000	200
WVTR/g m^{-2} per a day	0.434	0.254

of Fig. 7), and the time-dependent electrical performance of the devices was characterized. Fig. 7 shows that the transfer characteristic curves of OFETs before and after passivation at 90 °C were nearly identical. The value for μ increased from 1.3×10^{-2} to 1.4×10^{-2} cm^2 V^{-1} s^{-1}. Fig. 8(a) and (b) show device transfer characteristics with and without a passivation layer, stored in the dark and under ambient conditions (with a humidity of 60–80%) for 48 d. The OFETs without a passivation layer demonstrated

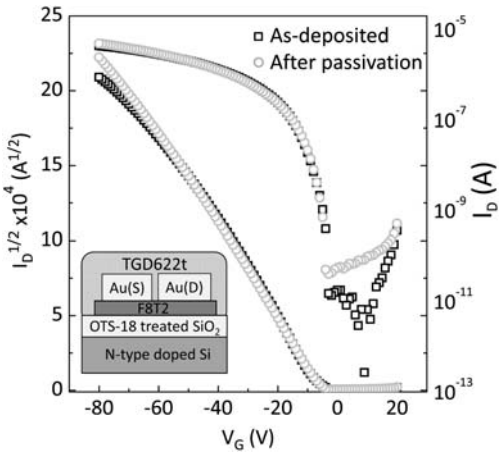

Fig. 7 The transfer characteristic curves of OFETs before and after TGD622t passivation cured at 90 °C. The inset shows a schematic representation of the OFETs.

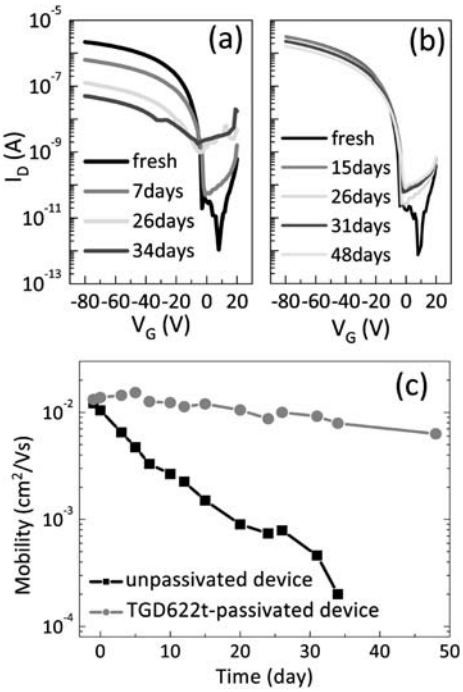

Fig. 8 Time-dependent I_D *versus* V_G characteristics of (a) unpassivated and (b) TGD622t-passivated OFETs. The I_D–V_G transfer curves were measured in the saturation regime. (c) Time-dependent changes of the field-effect mobility of unpassivated and TGD622t-passivated OFETs. All electrical measurements were performed in ambient air (with a humidity of 60–80%).

a mobility that was significantly lower than the initial mobility (μ_0), from 1.1×10^{-2} to 2.0×10^{-4} cm^2 V^{-1} s^{-1} (1.8% mobility relative to μ_0) after 34 d, as shown in Fig. 8(c). On the other hand, the passivated devices did not experience such significant mobility changes relative to the unpassivated devices, with an initial mobility of 1.3×10^{-2} and a final mobility of 8.0×10^{-3} cm^2 V^{-1} s^{-1} (60% mobility relative to μ_0) after 34 d. After 35 d, the unpassivated devices had nearly completely degraded, but the passivated devices still exhibited good electrical characteristics (45% mobility relative to μ_0 after 48 d, see Fig. 8(c)). As can be seen in Fig. 8(a) and 8(b), the changes in the on/off ratio ($I_{on/off}$) were much larger in devices without a passivation coating than in those with a passivation coating. In the unpassivated devices, water molecules in ambient air diffused into the grain boundaries of the polycrystalline semiconductor layer and/or the interface between the semiconductor and gate dielectric, thereby generating both donor- and acceptor-like traps and leading to a significant degradation of the electrical characteristics.[28]

Conclusions

In summary, an organic–inorganic hybrid passivation material that contained titania (TGD622t) was obtained by the solvent-free NH sol–gel method. After low-temperature curing, TGD622t formed a very dense and transparent film. The WVTR of solution-processed TGD622t films were 0.434 g m^{-2} per a day, indicating that it showed good barrier properties and was comparable to thermally-evaporated SiO_x film. Furthermore, TGD622t effectively protected the F8T2-based OFET devices from water molecules present in ambient air, resulting in OFETs that showed long-term stability relative to the unpassivated devices.

Acknowledgements

This work was supported by a grant from the Korea Science and Engineering Foundation (KOSEF) funded by the Korean Government (MEST) (20090079630),and by a grant from Information Display R&D Center as part of the Knowledge Economy Frontier R&D Program funded by the Ministry of Knowledge Economy of the Korean Government (F0004010-2008-31),and by the Korea Research Foundation Grant (KRF-2006-005-J01302).

References

1 D. Li, E.-J. Borkent, R. Nortrup, H. Moon, H. Katz and Z. Bao, *Appl. Phys. Lett.*, 2005, **86**, 042105.
2 Y. Wen, Y. Liu, C. Di, Y. Wang, X. Sun, Y. Guo, J. Zheng, W. Wu, S. Ye and G. Yu, *Adv. Mater.*, 2009, **21**, 1631.
3 K. Lee, J. Y. Kim, S. H. Park, S. H. Kim, S. Cho and A. J. Heeger, *Adv. Mater.*, 2007, **19**, 2445.
4 C. Charton, N. Schiller, M. Fahland, A. Holländer, A. Wedel and K. Noller, *Thin Solid Films*, 2006, **502**, 99.
5 H. Jeon, K. Shin, C. Yang, C. E. Park and S.-H. K. Park, *Appl. Phys. Lett.*, 2008, **93**, 163304.
6 N. Kim, W. J. Potscavage, Jr., B. Domercq, B. Kippelen and S. Graham, *Appl. Phys. Lett.*, 2009, **94**, 163308.
7 J. Meyer, P. Görrn, F. Bertram, S. Hamwi, T. Winkler, H.-H. Johannes, T. Weimann, P. Hinze, T. Riedl and W. Kowalsky, *Adv. Mater.*, 2009, **21**, 1845.

8 S. Nam, H. Jeon, S. H. Kim, J. Jang, C. Yang and C. E. Park, *Org. Electron.*, 2009, **10**, 67.
9 S. Cho, K. Lee and A. J. Heeger, *Adv. Mater.*, 2009, **21**, 1941.
10 M. D. Groner, S. M. George, R. S. Mclean and P. F. Carcia, *Appl. Phys. Lett.*, 2006, **88**, 051907.
11 H. Schmidt and H. wolter, *J. Non-Cryst. Solids*, 1990, **121**, 428.
12 K.-H. Haas, S. Amberg-Schwab, K. Rose and G. Schottner, *Surf. Coat. Technol.*, 1999, **111**, 72.
13 M. Popall, J. Kappel, M. Pilz, J. Schulz and G. Feyder, *J. Sol-Gel Sci. Technol.*, 1994, **2**, 157.
14 P. H. Mutin and A. Vioux, *Chem. Mater.*, 2009, **21**, 582.
15 K.-H. Nam, T.-H. Lee, B.-S. Bae and M. Popall, *J. Sol–Gel Sci. Technol.*, 2006, **39**, 255.
16 J. N. Hay and H. M. Raval, *Chem. Mater.*, 2001, **13**, 3396.
17 W.-S. Kim, K.-S. Kim, Y.-J. Eo, K. B. Yoon and B.-S. Bae, *J. Mater. Chem.*, 2005, **15**, 465.
18 Y. K. Kwon, J. K. Han, J. M. Lee, Y. S. Ko, J. H. Oh, H.-S. Lee and E. H. Lee, *J. Mater. Chem.*, 2008, **18**, 579.
19 D. Hoebbel, M. Nacken and H. Schmidt, *J. Sol–Gel Sci. Technol.*, 1998, **12**, 169.
20 S. S. Williams, M. J. Hampton, V. Gowrishankar, I.-K. Ding, J. L. Templeton, E. T. Samulski, J. M. DeSimone and M. D. McGehee, *Chem. Mater.*, 2008, **20**, 5229.
21 S. Yang, J. H. Kim, J. H. Jin and B.-S. Bae, *J. Polym. Sci., Part B: Polym. Phys.*, 2009, **47**, 756.
22 R. M. Almeida and C. G. Pantano, *J. Appl. Phys.*, 1990, **68**, 4225.
23 L. Téllez, J. Rubio, F. Rubio, E. Morales and J. L. Oteo, *J. Mater. Sci.*, 2003, **38**, 1773.
24 H. Yamashita, S. Kawasaki, Y. Ichihashi, M. Harada, M. Takeuchi, M. Anpo, G. Stewart, M. A. Fox, C. Louis and M. Che, *J. Phys. Chem. B*, 1998, **102**, 5870.
25 P. Innocenzi, G. Brusatin and F. Babonneau, *Chem. Mater.*, 2000, **12**, 3726.
26 W. Que, Y. Zhou, Y. L. Lam, Y. C. Chan and C. H. Kam, *Thin Solid Films*, 2000, **358**, 16.
27 D. L. Pavia, G. M. Lampman and G. S. Kriz, *Introduction to Spectroscopy*, Harcourt Inc., 3rd edn, 2001, Ch. 2, pp. 29–70.
28 S. H. Kim, H. Yang, S. Y. Yang, K. Hong, D. Choi, C. Yang, D. S. Chung and C. E. Park, *Org. Electron.*, 2008, **9**, 673.

